

Demonstration of diffraction enhancement via Bloch surface waves in *a*-SiN:H multilayers

Marco Liscidini,^{1,a)} Matteo Galli,² Maddalena Patrini,² Richard W. Loo,³ M. Cynthia Goh,³ Carlo Ricciardi,⁴ Fabrizio Giorgis,⁴ and J. E. Sipe¹

¹Department of Physics, University of Toronto, 60 St. George Street, Toronto, Ontario M5S 1A7, Canada

²Department of Physics "A. Volta," University of Pavia, Via Bassi 6, I-27100 Pavia, Italy

³Department of Chemistry, University of Toronto, 80 St. George Street, Toronto, Ontario M5S 3H6 Canada

⁴Department of Materials Science and Chemical Engineering, χ Lab-LATEMAR, Polytechnic University of Torino, C.so Duca degli Abruzzi 24, I-10129 Torino, Italy

(Received 4 December 2008; accepted 7 January 2009; published online 30 January 2009)

By exploiting the excitation of a Bloch surface wave at a wavelength $\lambda=670$ nm, we observe a diffraction enhancement of more than 45 times from a rabbit IgG protein grating printed on *a*-SiN:H multilayers. Our results demonstrate that the use of surface states in dielectric multilayers is very promising for the realization of the next generation of diffraction-based biosensors. © 2009 American Institute of Physics. [DOI: 10.1063/1.3076101]

Bloch surface waves (BSWs) are electromagnetic field excitations that are confined near the interface separating a photonic crystal (PhC) from a dielectric homogeneous medium, and which propagate along that interface.¹ In a BSW, the electromagnetic field is confined close to the PhC surface by the photonic gap, which prevents light propagation in the periodic structure, and by the total internal reflection, which results in an exponential decay of the field in the homogeneous medium.² BSWs can be considered the dielectric analogs of surface plasmons (SPs), although both the light confinement mechanism and a host of other properties are different for these two types of field excitations.³ In one-dimensional systems, BSWs exist for both transverse-electric (TE) and transverse-magnetic polarizations, unlike SPs, and their dispersion relations can be tailored by changing the structural parameters of the system. Moreover, since the use of metal is not required to fabricate a structure supporting BSWs, these excitations are free from absorption losses when transparent materials at the desired wavelength are considered. On the other hand, SPs allow light confinement well below the diffraction limit, an effect generally not observed in BSWs, where the field may extend into the PhC for several periods, depending on the refractive index contrast and the mode position in the photonic gap.⁴ Nonetheless, with the current development of plasmonic device for applications in the most diverse research fields, it is not surprising that there is a renewed interest in the study of BSWs,⁵⁻⁷ which have been known since the late 1970s.¹

The use of BSWs is particularly promising for application to optical biosensing, where the capability to guide and confine light in micro- and nanostructures can be exploited both to reduce detector size and to enhance sensitivity by increasing the effective light-matter interaction.⁸⁻¹² Of course, SP-based optical sensors have enjoyed great success because of their high sensitivity and ease of fabrication. Many of them exploit the strong dependence of the SP dispersion on the refractive index of the ambient at the metal surface. Small refractive index changes, induced, for example, by the adsorption of a molecule on the surface, can

lead to a shift in the SP that can be optically detected.⁹ Since the fabrication of multilayer dielectric structures is already a mature technology, the similarity between BSWs and SPs suggests that periodic dielectric stacks could, in certain cases, substitute for metal in many SP biosensors, leading to an improvement in sensitivity through a reduction of mode propagation losses.⁵

In a previous work,¹³ we proposed the use of BSWs to enhance the diffraction intensity from protein gratings typically used in diffraction-based biosensors. In these devices, the quadratic dependence of the diffraction intensity on the grating height is exploited to detect protein adsorption on the grating surface.¹⁴ The diffracted signal is usually very small—about 10^{-5} the intensity of the specularly reflected light—and thus light confinement strategies to increase the interaction time between the light and the grating, using SPs or BSWs, can lead to an important enhancement of the diffraction signal.¹⁵

In this work, we demonstrate diffraction enhancement for a protein grating printed on an amorphous silicon nitride (*a*-Si_{1-x}N_x:H) multilayer when a BSW is excited by the incident beam. The observed signal intensity of the first diffraction order (-1) is more than 45 times larger than that produced by the same grating when fabricated directly on a glass substrate [see Fig. 1(a)].

The sample structure is an *a*-Si_{1-x}N_x:H multilayer, grown by plasma enhanced chemical vapor deposition on a 7059 Corning glass substrate.^{16,17} The first layer is 32 nm of *a*-Si_{0.45}N_{0.55}:H followed by seven periods of a unit cell composed of 145 nm of *a*-Si₃N₄:H and 135 nm of *a*-Si_{0.45}N_{0.55}H. A protein grating is applied to the first layer of the sample by microcontact printing, using a polydimethylsiloxane stamp inked with 40 μ l of 50 μ g/ml rabbit IgG in phosphate buffered saline (PBS) solution, as illustrated in Ref. 14. The final grating is about 4 nm high, with a period $\Lambda \cong 4.85$ μ m and air fraction $f \cong 0.5$, as confirmed by atomic force microscopy (AFM) images shown in Figs. 1(b) and 1(c).

In Fig. 2, we show the dispersion relation in the *x* direction of the TE-polarized BSW for the corresponding infinite *a*-Si_{1-x}N_x:H multilayer. The surface mode lies below the air light line and within the photonic band gap. The position of

^{a)}Electronic mail: liscidini@physics.utoronto.ca.

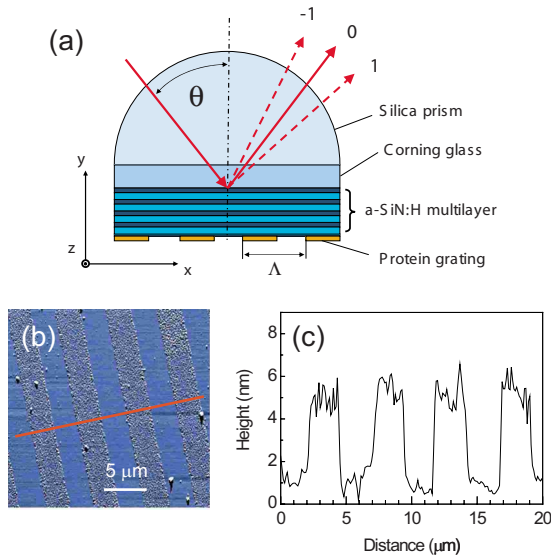


FIG. 1. (Color online) (a) Sample and ATR experiment scheme. (b) AFM error signal image of the protein grating printed on the top of the $a\text{-Si}_{1-x}\text{N}_x\text{:H}$ sample. (c) Height profile of the protein grating along the red line on panel (b).

the photonic gap depends on the material refractive indices and the unit cell composition, but not on the homogeneous medium properties nor on the thickness of the first layer. In this sense, the photonic gap can be considered a bulk property of the truncated PhC. On the other hand, the dispersion of the surface mode is strongly affected by the external medium refractive index and by the dielectric stack termination. Our goal here is to demonstrate diffraction enhancement in air at a wavelength of $\lambda=670$ nm. Nonetheless, we designed the multilayer to work over a wide frequency range and with different external media, such as water-based physiological solutions suitable for biological assays, with a higher refractive index that would result in a light line lower than that of the air. In the design, it is also important to consider that the real structure is finite and grown on a Corning 7059 substrate ($n=1.55$ at $\lambda=670$ nm), the thickness of which is typically

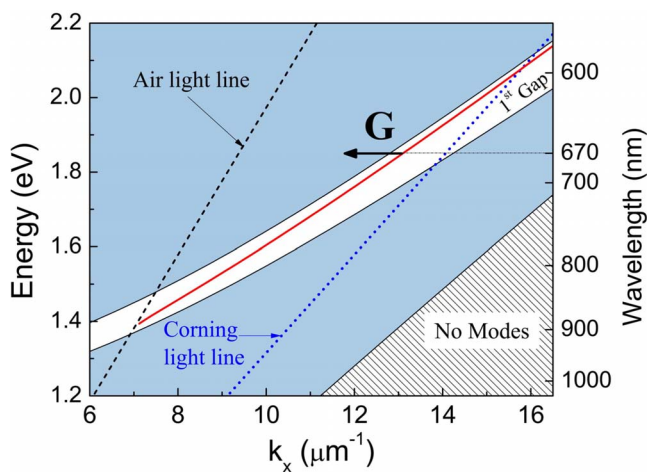


FIG. 2. (Color online) TE BSW dispersion (solid red) for a $a\text{-Si}_{1-x}\text{N}_x\text{:H}$ multilayer. The unit cell is composed of 135 nm of $a\text{-Si}_{0.45}\text{N}_{0.55}\text{:H}$ and 145 nm of $a\text{-Si}_3\text{N}_4\text{:H}$. The first layer is 32 nm of $a\text{-Si}_{0.45}\text{N}_{0.55}\text{:H}$. The external medium is air ($n=1$). The length of the vector G represents the momentum contribution provided by a one-dimensional grating of period $\Lambda=4.85$ μm . Light lines for air (dashed black) and Corning 7059 ($n=1.55$) (dotted blue) are shown.

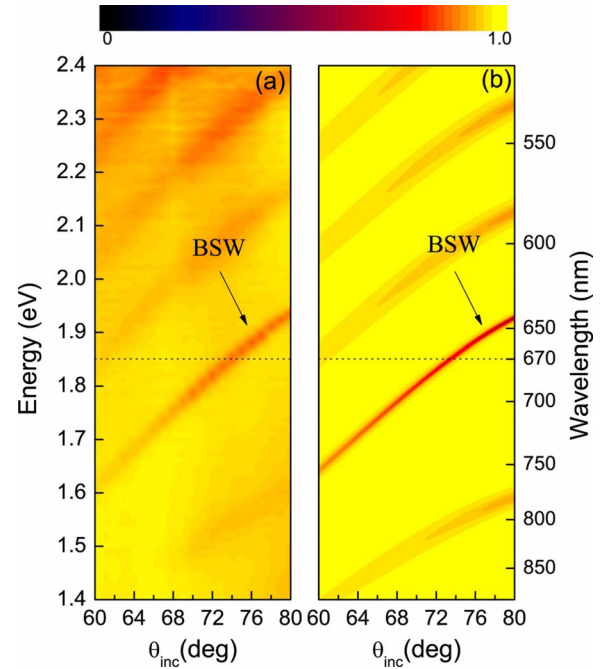


FIG. 3. (Color online) Experimental (a) and theoretical (b) ATR spectra as a function of the angle of incidence for the $a\text{-Si}_{1-x}\text{N}_x\text{:H}$ multilayer with $N=7$ periods. The unit cell is composed of 135 nm of $a\text{-Si}_{0.45}\text{N}_{0.55}\text{:H}$ and 145 nm of $a\text{-Si}_3\text{N}_4\text{:H}$. The first layer is 32 nm of $a\text{-Si}_{0.45}\text{N}_{0.55}\text{:H}$. The external medium is air ($n=1$), and the ATR spectra are taken in Kretschmann configuration using a hemispherical silica prism.

1–2 mm. In this structure, one is able to excite the BSW in the Kretschmann configuration (that is, exciting from the Corning side) only when the mode is above the substrate light line, so the field can propagate in the substrate. Hence in the finite structure, the BSW is more accurately described as a leaky mode. The refractive index contrast in the multilayer is small ($\Delta n \cong 0.19$ at $\lambda=670$ nm), and in such structures the use of BSWs leads to great flexibility in the design. Indeed, here the confinement mechanism in the multilayer is based on the photonic gap and does not rely completely on total internal reflection as it would in a slab waveguide.

The multilayer was characterized before and after the grating fabrication by means of wavelength- and angle-resolved attenuated total internal reflection (ATR) measurements¹⁸ performed in the Kretschmann configuration using a silica hemisphere [see Fig. 1(a)]. This allows us to excite the BSW mode of the structure for different angles of incidence, thus mapping out the dispersion relation of the mode. Our structure can be thought of as a multilayer waveguide, and so in addition to the BSW, there are modes that lie outside of the photonic gap and are confined in the structure by simple total internal reflectance. When a mode is excited, scattering and absorption losses are enhanced due to the field localization in the structure, and we observe a decrease in the reflected light.

The experimental (a) and theoretical (b) ATR results are shown in Fig. 3. The calculations are performed using a standard Fourier modal method, where we take into account the dispersion in the refractive index.¹⁹ In this frequency range, material absorption can almost be neglected, but we have to consider scattering losses at the multilayer interfaces. We describe these by introducing a small imaginary part to the effective silicon nitride dielectric function ($\epsilon = \epsilon_1 + i\epsilon_2$). In

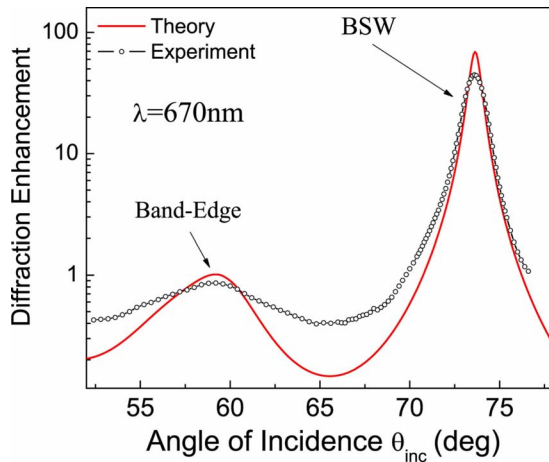


FIG. 4. (Color online) Experimental (points) and theoretical (solid line) diffraction enhancement as a function of the angle of incidence of the first diffraction order ($m=-1$) for a protein grating ($n=1.45$) of height $h=4$ nm and period $\Lambda=4.85$ μm printed onto the $a\text{-Si}_{1-x}\text{N}_x\text{:H}$ multilayer with $N=7$ periods. The diffraction enhancement is evaluated with respect to the case of the same protein grating printed on a 7059 substrate. The external medium is air ($n=1$) and the BSW is excited in Kretschmann configuration using a hemispherical silica prism.

line with the phenomenological nature of this description, we assume ε_2 to be independent of the wavelength and the silicon concentration, and we determine its value through a fit of the experimental data at $\lambda=670$ nm. We find that with a value of $\varepsilon_2=0.5 \times 10^{-3}$, we obtain good agreement between experimental results and the theoretical calculation. Note that such a small absorption affects only the width of the resonances but not their position. In a future communication, we plan to turn to a more realistic description of the effects of scattering on the spectrum.

To establish a reference for our experiments, the same deposition technique was used to imprint a grating on a bare Corning substrate. To calculate a diffraction enhancement factor, we divided the diffraction intensity of the multilayered system by that obtained with the simple Corning substrate. The enhancement for the first backward diffraction order (i.e., $k_d=k_{\text{inc}}-G$, where k_d and k_{inc} are the wave vectors components along \hat{x} of the diffracted and incident beams, respectively, and G is the momentum contribution provided by the grating) is plotted in Fig. 4 as a function of the angle of incidence at a wavelength of $\lambda=670$ nm. We also show the theoretical diffraction enhancement, calculated using the Fourier modal method where no fitting parameters are used. Both the experimental and theoretical curves show two peaks, at $\theta=59.2^\circ$ and $\theta=73.6^\circ$, that correspond to the band edge and the BSW mode, respectively. When the BSW is excited, the field is highly localized at the multilayer surface

and the measured diffraction intensity is 46 times larger than for the reference sample. In the stop band, between 60° and 70° , the diffraction is suppressed by the multilayer reflectance, which limits the interaction between the incoming beam and the grating. Although an enhancement is expected at the band edge, especially when the number of periods is large, this is in general less than when a BSW is excited, since at the band edge the field is distributed in the whole multilayer and not localized near the grating.¹³ In this structure, which has a small dielectric contrast and is composed of seven periods, there is no advantage to work at the band edge. The experimental trends are predicted by the theory, where our phenomenological treatment of scattering effects, although approximate, gives qualitative agreement with experiment.

In conclusion, we have demonstrated a 45-fold enhancement in the diffraction efficiency at $\lambda=670$ nm of a thin (4 nm high) protein grating imprinted on an $a\text{-Si}_{1-x}\text{N}_x\text{:H}$ multilayer. This enhancement is due to the strong field localization at the surface of the structure when a BSW is excited. Since an enhancement of the diffracted signal leads to an increase in device sensitivity,^{4,15} our results confirm that the use of structures supporting BSWs may find important application in the field of diffraction-based biosensors.

This work was supported by the Ontario Center of Excellence, LATEMAR Network, and Axela Inc.

- ¹P. Yeh, A. Yariv, and A. Y. Cho, *Appl. Phys. Lett.* **32**, 104 (1978).
- ²A. Yariv and P. Yeh, *Optical Waves in Crystals* (Wiley, New Jersey, 2003).
- ³W. L. Barnes, *J. Opt. A, Pure Appl. Opt.* **8**, S87 (2006).
- ⁴M. Liscidini and J. E. Sipe, *J. Opt. Soc. Am. B* **26**, 279 (2009).
- ⁵M. Shinn and W. M. Robertson, *Sens. Actuators B* **105**, 360 (2005).
- ⁶E. Guillermain, V. Lysenko, R. Orobtcouk, T. Benyattou, S. Roux, A. Pillonnet, and P. Perriat, *Appl. Phys. Lett.* **90**, 241116 (2007).
- ⁷T. Sfez, E. Descrovi, L. Dominici, W. Nakagawa, F. Giorgis, and H. Herzig, *Appl. Phys. Lett.* **93**, 061108 (2008).
- ⁸O. S. Wolfbeis, *Anal. Chem.* **72**, 81 (2000).
- ⁹J. Homola, *Anal. Bioanal. Chem.* **377**, 528 (2003).
- ¹⁰J. J. Saarinen, S. M. Weiss, P. M. Fauchet, and J. E. Sipe, *Opt. Express* **13**, 3754 (2005).
- ¹¹A. M. Armani, R. P. Kulkarni, S. E. Fraser, R. C. Flagan, and K. J. Vahala, *Science* **317**, 783 (2007).
- ¹²A. Nitkowski, L. Chen, and M. Lipson, *Opt. Express* **16**, 11930 (2008).
- ¹³M. Liscidini and J. E. Sipe, *Appl. Phys. Lett.* **91**, 253125 (2007).
- ¹⁴J. B. Goh, R. W. Loo, R. A. McAloney, and M. C. Goh, *Anal. Bioanal. Chem.* **374**, 54 (2002).
- ¹⁵F. Yu, S. Tian, D. Yao, and W. Knoll, *Anal. Chem.* **76**, 3530 (2004).
- ¹⁶F. Giorgis, *Appl. Phys. Lett.* **77**, 522 (2000).
- ¹⁷C. Ricciardi, V. Ballarini, M. Galli, M. Liscidini, L. C. Andreani, M. Losurdo, G. Bruno, S. Lettieri, F. Gesuele, P. Maddalena, and F. Giorgis, *J. Non-Cryst. Solids* **352**, 1294 (2006).
- ¹⁸M. Galli, M. Belotti, D. Bajoni, M. Patrini, G. Guizzetti, D. Gerace, M. Agio, L. C. Andreani, and Y. Chen, *Phys. Rev. B* **70**, 081307 (2004).
- ¹⁹D. M. Whittaker and I. S. Culshaw, *Phys. Rev. B* **60**, 2610 (1999).